

Therapeutic Ratio Quantifies Laser Antisepsis: Ablation of *Porphyromonas gingivalis* With Dental Lasers

David M. Harris, PhD^{1,2*} and Michael Yessik, PhD³

¹Bio-Medical Consultants, Inc., 4256 Heyer Avenue, Castro Valley, California

²Department of Preventative and Restorative Dental Sciences, University of California, San Francisco, California

³Incisive, LLC, Richmond, California

Background and Objectives: It is established that both pulsed Nd:YAG (1,064 nm) and continuous diode (810 nm) dental lasers kill pathogenic bacteria (laser antisepsis), but a quantitative method for determining clinical dosimetry does not exist. The purpose of this study was to develop a method to quantify the efficacy of ablation of *Porphyromonas gingivalis* (*Pg*) in vitro for two different lasers.

Study Design/Materials and Methods: The ablation thresholds for the two lasers were compared in the following manner. The energy density was measured as a function of distance from the output of the fiber-optic delivery system. *Pg* cultures were grown on blood agar plates under standard anaerobic conditions. Blood agar provides an approximation of gingival tissue for the wavelengths tested in having hemoglobin as a primary absorber. Single pulses of laser energy were delivered to *Pg* colonies and the energy density was increased until the appearance of a small plume was observed coincident with a laser pulse. The energy density at this point defines the ablation threshold. Ablation thresholds to a single pulse were determined for both *Pg* and for blood agar alone.

Results: The large difference in ablation thresholds between the pigmented pathogen and the host matrix for pulsed-Nd:YAG represented a significant therapeutic ratio and *Pg* was ablated without visible effect on the blood agar. Near threshold the 810-nm diode laser destroyed both the pathogen and the gel.

Conclusions: Clinically, the pulsed Nd:YAG may selectively destroy pigmented pathogens leaving the surrounding tissue intact. The 810-nm diode laser may not demonstrate this selectivity due to its greater absorption by hemoglobin and/or longer pulse duration. *Lasers Surg. Med.* 00:1–8, 2004. © 2004 Wiley-Liss, Inc.

Key words: periodontitis; diode Nd:YAG dental laser; bacterial reduction; laser antisepsis; *P. gingivalis*

INTRODUCTION

Several reports indicate that laser sulcular debridement using the pulsed Nd:YAG dental laser with scaling and root planning leads to improvement in clinical indices [1–3], and, when adjunctive to a total treatment plan [4,5] may lead to regeneration of periodontal supporting structures [6–8]. In clinical studies, where pockets and root canals are sampled for bacterial content before and after Nd:YAG or

diode laser treatment, there are consistent observations of bacterial reduction [1,9–24]. The species most affected seem to be *Porphyromonas gingivalis* (*Pg*), *Prevotella intermedia*, and other dark-pigmented bacilli. It is likely that the efficacy of the laser treatment is related to eradication of certain species of oral pathogens from the periodontal tissues [23].

Need to Quantify Dosimetry

In vitro culture and tissue models provide an opportunity to control irradiances and measure pathogen ablation dynamics. Schultz et al. [23] placed bacterial suspensions in 6-mm wells and irradiated them with a 20–120 W continuous wave Nd:YAG laser. They measured viable cell counts after serial dilutions of *Escherichia coli*, *Pseudomonas aeruginosa*, and *Staphylococcus aureus* and achieved significant reductions with a dose/response relationship. Unfortunately, because of calibration problems actual surface irradiances are not available from the paper. Tseng et al. [20,24] irradiated 3-mm diameter colonies and extracted root surfaces with 150-microseconds pulsed Nd:YAG. Samples from irradiated areas were reinoculated and rate of regrowth was used to estimate bactericidal activity. Regrowth of black-pigmented wild strain bacteriodes were markedly reduced with dose dependence. The threshold for the effect was in the range 25–130 J/cm². Whittiers et al. 1994 [22] irradiated nine species of pathogens in suspensions, including *Pg*, with pulsed Nd:YAG. During irradiation they stirred the broth with the fiber tip for 1–4 minutes and measured colony-forming units from irradiated and control samples. All nine species exhibited dose-dependent responses, although absolute fluences are unknowable.

Most laser bactericidal studies report that a dose/response function exists. That is, dental lasers destroy bacteria and, as one turns up the wattage, more bacteria are killed. Regrettably, irradiances are usually not available

*Correspondence to: David M. Harris, PhD, Bio-Medical Consultants, Inc., 4256 Heyer Ave, Castro Valley, California 94546. E-mail: bmcinc@comcast.net

Accepted 14 June 2004

Published online in Wiley InterScience
(www.interscience.wiley.com).

DOI 10.1002/lsm.20086

due to inaccurate or absent reporting of parameters. Also, some investigators used a “sweeping motion” during treatment [1,11,15] and the angle of irradiation could vary from 0° to 90° making computation of fluence impossible. We conclude that there is a need for accurate and repeatable measures of specific levels of irradiation and their bactericidal and tissue effects. Such measurements are attainable in vitro using well-calibrated instrumentation.

Objectives

We have selected *P. gingivalis* as the initial target pathogen to develop our methodology since it is implicated as necessary and synergistic to periodontal disease. The objectives of this study were to quantify laser ablation of *Pg* in vitro for both cw-diode and pulsed-Nd:YAG dental lasers, and to evaluate the selectivity of *Pg* destruction using an in vitro tissue model. The results provide a framework for defining an efficacious clinical dosimetry for laser antisepsis.

MATERIALS AND METHODS

Lasers

Two dental laser systems were used in this study (Fig. 1). A 6-W InPulse™ Nd:YAG (1,064 nm) Dental Laser (Incisive, LLC, Fremont, CA) delivered 1,064-nm pulses to the samples through a 320 μ m optical fiber. The Nd:YAG had a free-running pulse width of 100 microseconds with variable energy per pulse of 20–200 mJ. Pulse timing was controlled electronically by replacing the foot switch with a digital timer (National Controls Corp., TMM Multifunction Relay). Typically, single 100-microseconds duration, 100-mJ pulses were delivered in these experiments. A 6-W continuous-Wave DioLase ST™ Diode (810-nm) Dental Laser System (American Dental Laser Technology, Inc., Corpus Cristi, TX) had a similar fiberoptic delivery system. Uniform 100-millisecond duration pulses were obtained by use of the digital timer instead of the foot switch.

Laser Calibration

The laser beams were characterized by collecting beam profiles at various distances from the distal fiber tip. The beam was directed into an NIST-calibrated energy/power meter (Ophir, DGX) and a straight edge was stepped across the beam. Profiles were constructed by measuring the change in energy between steps. Profiles of the Nd:YAG beam at 2- and 4-mm from the tip (320- μ m fiber) are shown in Figure 2A. From these functions we estimate the beam radius as the x value where $y = 1/e^2$ of the peak irradiance. Beam radii are plotted in Figure 2B for both the 810-nm diode and the 1,064-nm pulsed Nd:YAG. The least squares best-fit regression estimates the divergence of the beam and provides a computational formula for determining the spot size at any distance from the fiber tip.

The average fluence at any target distance is equal the total energy in the beam (measured with the power meter) divided by the spot area (πr^2) at that distance. It is necessary to specify ablation thresholds with the peak fluence because ablation occurs first in the center of the beam where the energy density is greatest. For a Gaussian beam, the peak is exactly equal to two times the average. Peak fluence as a function of target distance can be computed from these measurements. Shown in Figure 2C is the function for a 93-mJ pulse from the Nd:YAG and a 389-mJ pulse from the diode.

Bioassay

The bioassay set-up diagrammed in Figure 3 was used to determine the sensitivity of bacteria in culture to laser irradiation. *Pg* colonies in situ in the petri dish were placed in the beam path, the fiber tip was lowered to the culture surface and the stepper motor readout (2- μ m steps) was set to zero. Fiber tip distances above the culture surface were converted to peak irradiances using the calibration described above. Target tissues were irradiated with single pulses under direct observation with 40 \times video magnification.

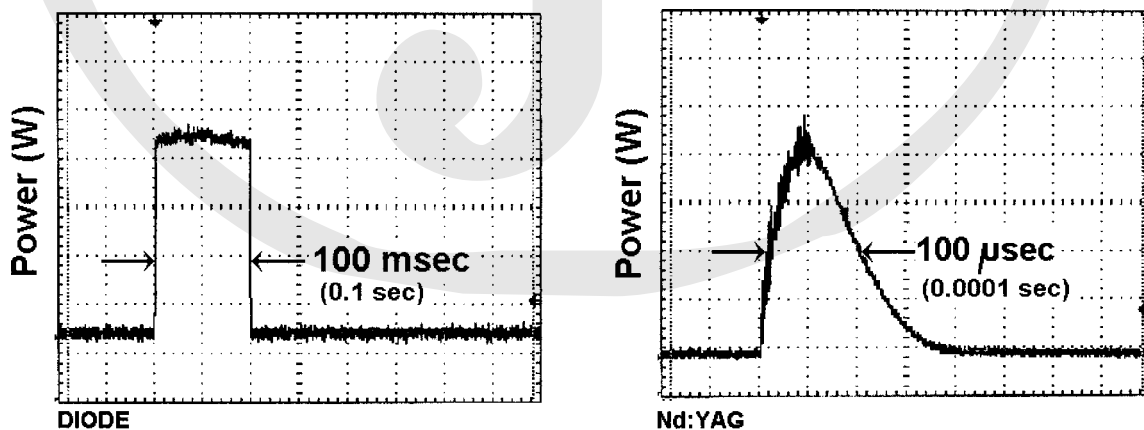


Fig. 1. Temporal characteristics of pulses emitted from pulsed Nd:YAG and gated diode dental lasers. Light reflected from the target was sensed with a THORLABS DET110 high-speed silicon photodetector and stored with a Tektronix TDS 1002 digital storage oscilloscope.

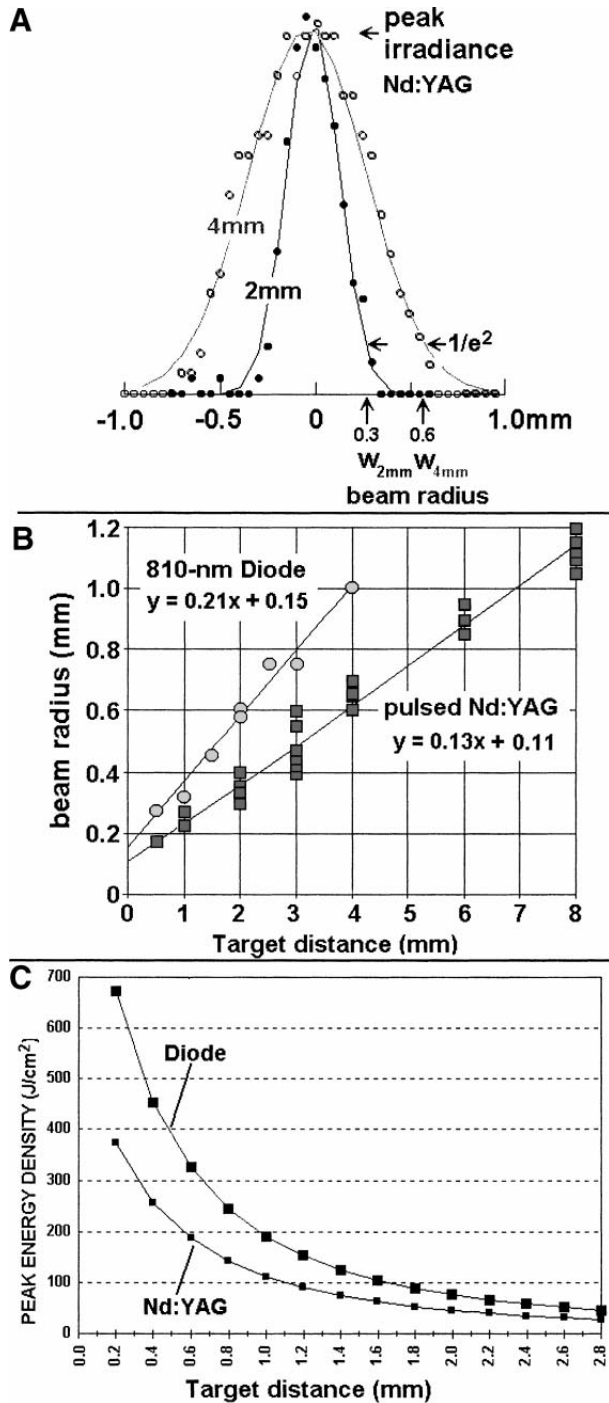


Fig. 2. **A**: Beam profiles of pulsed Nd:YAG at 2- and 4-mm from the tip. **B**: Beam radius as a function of target distance for pulsed Nd:YAG and 810-nm diode dental lasers. **C**: Peak fluence versus target distance for Nd:YAG and diode.

Pg Colonies

In a level 2 microbiology laboratory at UCSF stock cultures of *P. gingivalis*, 33277 were maintained by anaerobic culture (85% N_2 , 10% H_2 , and 5% CO_2) at 37°C on LRBB

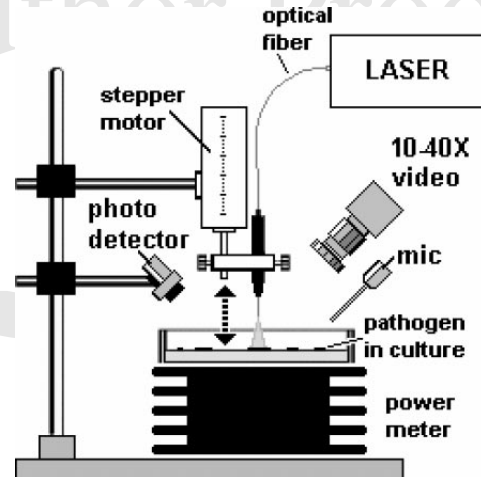


Fig. 3. Diagram of bioassay. *P. gingivalis* grown on blood agar in petri dishes is placed in the beam path. Irradiance is determined by positioning the fiber tip with a stepper motor (2- μ m). Ablation thresholds are determined by direct video observation at 40 \times magnification.

agar (*Brucella* agar base supplemented with 5% laked rabbit blood, 2.5 μ g/ml hemin, 5.0 μ g/ml menadione, and 0.01% dithiothreitol). Colonies form a 30–60 μ m thick bio-film on the agar surface (Fig. 4B). The blood agar containing water, hemoglobin, and other organics, approximates the optical properties of soft tissue.

Ablation Threshold

Ablation (removal of tissue) occurs when photons are absorbed by the target and the resulting temperature increase is sufficient to vaporize or thermally coagulate tissue within the laser beam (it is assumed that vaporization and coagulation are processes that are bacteriocidal). A basic physical characteristic of tissue ablation by laser energy is: as radiant exposure increases, the depth of tissue removal increases [25]. Very low level exposure has no immediate visible effect and there is a threshold energy dose necessary to ablate a just measurable amount of tissue. For laser antiseptis, the threshold fluence that is lethal to the target pathogen is defined by this minimum, the ablation threshold. This is significant since ablation threshold defines a radiant exposure that is toxic to the target pathogen at or above this value. Thus, laser ablation of *Pg* is an example of laser antiseptis (elimination of microorganisms that cause disease).

We use a visual detection method to identify ablation thresholds. Fluence (J/cm^2) is varied by advancing or retracting the fiber tip from the surface of the *Pg* colony with the 2- μ m stepper motor. Each laser pulse is delivered to a fresh spot on the colony to avoid cumulative effects. When a pulse is delivered the following observations are made from the video microscope monitor. At high fluences each pulse creates an obvious plume and crater (Fig. 4A). At lower fluences, a smaller plume and blanching appears

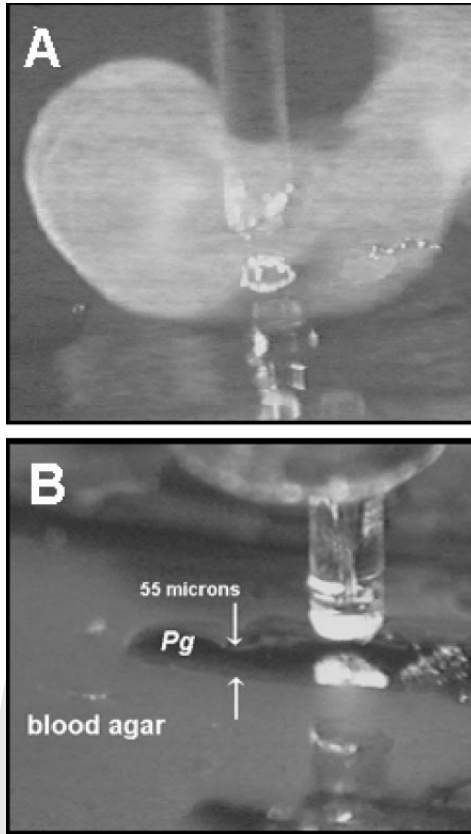


Fig. 4. **A:** Plume emitted from the surface of a *Pg* colony following a 230 J/cm^2 pulse from the Nd:YAG. **B:** Colonies of *Pg* cultured on rabbit blood agar form a $30\text{--}80 \text{ }\mu\text{m}$ thick biofilm that expands across the agar surface.

in the center of the beam on the target surface. As the energy is decreased the blanched area observed decreases in size, indicating less material removed. About 5-J/cm^2 below the threshold of the “surface blanching effect” a small plume of ablated material is still emitted from the target surface. At lower energies there is no visible effect. The fluence level between these last two observations defines ablation threshold. Several series of increasing and decreasing fluences were measured for each colony and the median ablation threshold was recorded. A similar technique was employed to measure the ablation threshold of blood agar alone.

RESULTS

Selective Ablation

Figure 5 shows ablation craters in *Pg* colonies made with single 1 mm diameter, 217-mJ/cm^2 peak fluence pulses from the Nd:YAG. Notice the Nd:YAG craters have a flat bottom indicating that no agar was ablated. The pulse selectively vaporized all bacteria from within the laser spot, but left the substrate blood agar intact.

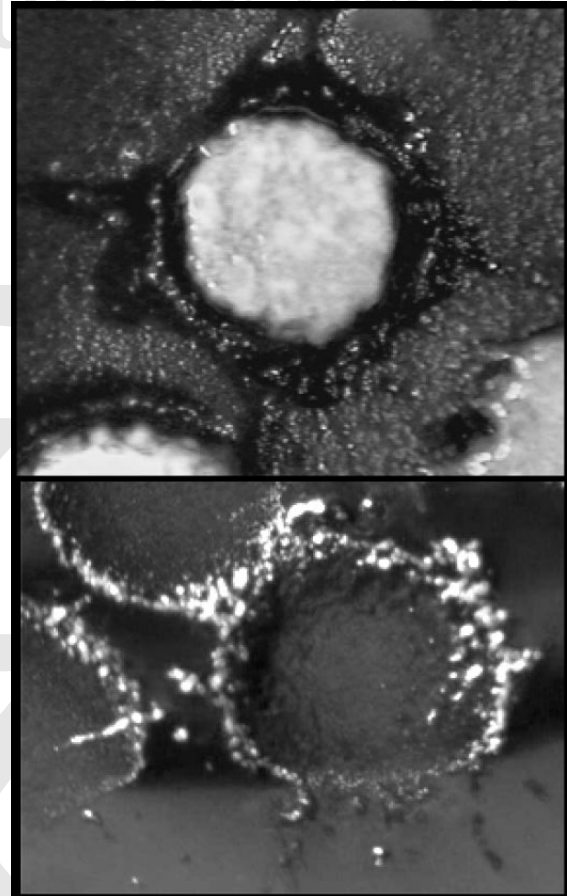


Fig. 5. Craters in *Pg* colonies by pulsed Nd:YAG. It is obvious that the laser energy destroyed the bacteria (1-mm diameter spot). Notice at the bottom that the craters have a relatively flat bottom and that the Nd:YAG laser did not appear to affect the blood agar.

Ablation Thresholds of *Pg* and Laked Rabbit Blood Agar

Average ablation thresholds for *Pg* determined for the Nd:YAG was 48-J/cm^2 ($N=12$) and for the diode, 96-J/cm^2 ($N=9$). Ablation threshold of blood agar alone determined for the diode was 146-J/cm^2 . The Nd:YAG had no visible effect on blood agar alone at the highest peak energy density available ($1,700\text{-J/cm}^2$).

One experimental trial is illustrated in Figure 6. A series of craters in *Pg* colonies on blood agar were made with single pulses at the indicated irradiances for the two lasers. For this sample the ablation threshold determined with the plume detection method was 50-J/cm^2 for the Nd:YAG and 94-J/cm^2 for the diode. Notice in Figure 6 that the diode craters do not have a flat bottom but were Gaussian in shape and included removal of both *Pg* and agar. Figure 7 shows two series of impacts on blood agar alone. The sample was slightly dehydrated to improve image contrast. The diode laser had an effect on the agar at and above fluences of

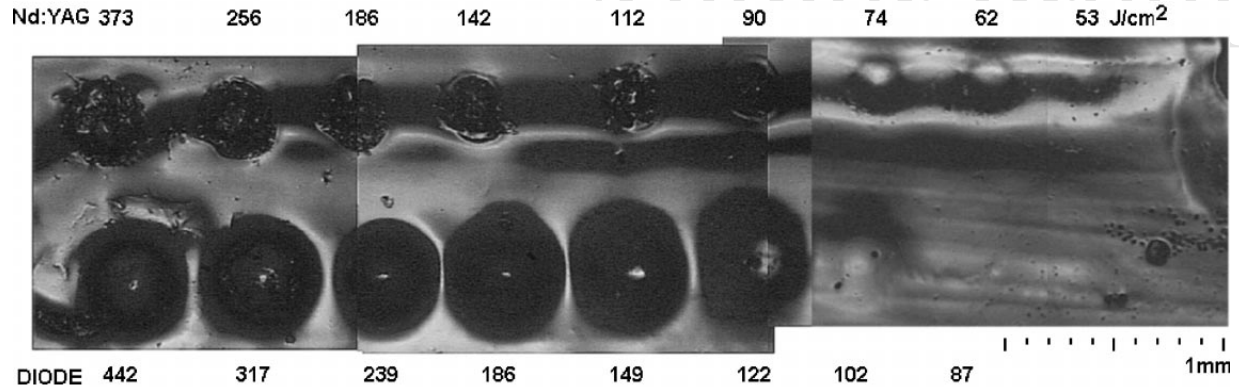


Fig. 6. Series of craters in *Pg* colonies on blood agar below were made by a series of single pulses at the indicated irradiances for the two lasers.

92-J/cm², but there was no visible effect of Nd:YAG pulses up to 1,148-J/cm².

DISCUSSION

Selective Ablation

At 1,064-nm the absorption by the pigments in *Pg* is greater than absorption by hemoglobin or water in the gel. Therefore, laser energy is preferentially absorbed within *Pg* and not by the blood agar. We were unable to ablate the agar alone at the maximum irradiation capable with the Nd:YAG laser system. These data illustrate the concept of selective ablation of *Pg* in this tissue model.

Therapeutic Index for Drugs Adapted to Antibiotic Laser

The concept of selectivity is an essential element in the current framework of chemical antibiotic treatment. The selectivity of a drug that destroys pathogens but is benign to

normal tissue is expressed as the ratio of the drug concentration (mg/kg) that is toxic to normal tissue (toxic dose) to the drug dose that is toxic to the target pathogen (therapeutic dose). This is referred to as the therapeutic ratio or therapeutic index. A high value for the index indicates high selectivity.

The laser bioassay was developed to evaluate the sensitivity of *P. gingivalis* to the antibiotic action of the laser. For laser antiseptic, the threshold irradiance that is lethal to the target pathogen has been defined as the ablation threshold, the minimum energy density (J/cm²) necessary to remove a just detectable amount of pathogen. In analogy with antibiotic nomenclature, we can determine the therapeutic index to treatment of specific pathogens by specific laser systems. In this case, the therapeutic dose (A) is defined as the minimum laser fluence that destroys pathogens and the toxic dose (B) as the fluence damaging to normal tissues. The therapeutic index is calculated as the ratio: B/A. The therapeutic indices for the *Pg*-agar tissue model are diode: 1.5 and Nd:YAG: > 24 (Table 1).

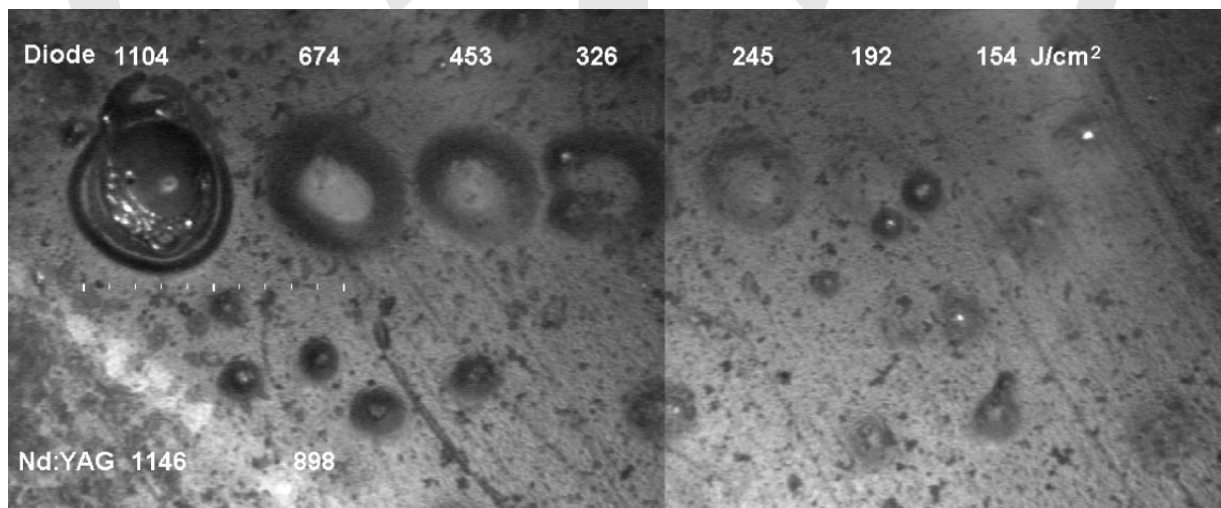


Fig. 7. Series of impacts on blood agar alone. Ablation threshold for blood agar was > 1,146-J/cm² for the pulsed Nd:YAG and < 192-J/cm² for the diode.

TABLE 1. Peak Energy Density (J/cm²) for Ablation Thresholds of *Pg* and Agar-Alone

	Diode	Nd:YAG
Blood agar	146	> 1,400
<i>P. gingivalis</i>	96	58
Therapeutic index	1.52	> 24

Average of 12 measurements for Nd:YAG and 9 for diode. The therapeutic index is the ratio (B/A) of the therapeutic light dose (A) necessary to destroy pathogens and the toxic dose (B) as the fluence damaging to normal tissues.

Depth of Laser Antisepsis

There is a “therapeutic and diagnostic window” in biological tissues where light absorption is minimal and light transmission is greatest [26,27]. This window is in the red to near-infrared region, approximately 800–1,200-nm, with maximum transmission for wavelengths close to 1,064-nm. At these wavelengths, if surface fluence is less than the surface damage threshold, then there remains a volume of tissue below the surface wherein energy deposition is lethal to pigmented bacteria. It follows that a greater therapeutic index means a greater potential depth of antisepsis. Because pulsed-Nd:YAG has a high therapeutic index the surface radiant exposure can be maintained below the toxic dose and a therapeutic dose can be delivered deep into the tissues. Diode lasers may be less effective due to their lower therapeutic index. The 810-nm diode laser may demonstrate lower selectivity than pulsed Nd:YAG due to its greater absorption by hemoglobin and/or longer pulse duration. In clinical practice penetration of diode laser energy into tissue is further hampered by the custom of “initiating” the distal end of the fiber. This procedure involves placing a light absorbent material on the tip causing the tip to heat up and, thus, increase its incisional efficiency. However, this also blocks emission and significantly decreases the surface radiant exposure.

Pg Persists by Evading Immune Effectors

Pg is a pigmented, Gram-negative, motile, anaerobic bacteria known to cause tissue destruction by release of proteinases [28,29] and lipopolysaccharides [30]. *Pg* has been established as a pathogenic bacteria involved in the periodontal disease process [31,32]. Eradication of *Pg* is important because *Pg* may be synergistic to disease progression [33,34]. *Pg* persists in the mixed-species plaque

biofilm on tooth surfaces and adheres to and enters epithelial cells [32,35–37] and inactivates PMNs [38]. Intracellular bacteria can evade host immune effectors and antibiotics commonly used to treat infection. Subgingival pathogenic bacteria tend to colonize stagnant ecological niches, or privileged sites [30], such as surface irregularities that favor retention and growth [39]. *Pg* is also known to colonize calculus and cementum, and penetrate into dentinal tubules and lacunae [40,41]. *Pg* is mostly concentrated attached to the biofilm surface [42], although it has been identified migrating far as 1-mm into the dentinal tubules [30,40].

These bacterial reservoirs are sources for recolonization of treated root surfaces. Since they are not eliminated by conventional mechanical treatment, it has become appropriate to combine mechanical periodontal therapy with the use of chemical antibiotics [40]. Antimicrobial agents, as adjuncts to conventional periodontal therapy, may be administered systemically or applied locally into the periodontal pocket. Antimicrobials may help to reduce the number of microorganisms within the periodontal pocket to levels lower than may be achieved with scaling alone but have limited access to privileged sites. Tetracycline and chlorhexadine have been shown to not penetrate much past the cementodentin junction [43,44] and intra-root canal antibiotic irrigants penetrate only a few 100- μ into the surrounding dentin [45]. Chemical antibiotics have additional disadvantages that include: potential allergic reactions, possible induction of drug resistance and systemic side effects. Furthermore, long term efficacy of local delivered antimicrobials has not been established.

Laser Antisepsis Versus Chemical Antibiotics

The laser mode of antisepsis has several potential advantages over traditional biochemical antibiotics in root disinfection (Table 2).

- (1) A therapeutic dose can be delivered to a greater depth immediately and leaves no residual concentration.
- (2) Laser radiation affects equally extracellular and intracellular pigmented pathogens and can access other privileged sites such as calculus and dentinal tubules.
- (3) Laser antisepsis has no known systemic side-effects, resistances, or negative interactions with other modes of therapy.
- (4) Laser energy has the potential to breach the protective mechanisms of biofilms [46].

TABLE 2. Comparison of Characteristics of Chemical Antibiotics (Drugs) Versus Laser Antisepsis

	Drugs	Laser
Side effects	Systemic	None
Resistance	Yes	No (albino mutant?)
Negative interactions	Possible	None
Spectrum of activity	Broad or narrow	Pigmented pathogens
Local delivery mode	Chemical dissolution	Light diffusion

Clinical Significance

When used for sulcular debridement and other dental treatments, the 100-microseconds pulsed Nd:YAG may selectively destroy pigmented pathogens to a depth below the tissue surface leaving the surrounding tissue intact.

ACKNOWLEDGMENTS

We thank Peter Loomer, DDS, (UCSF, Stomatology) for providing facilities during pilot experiments. Donald Layman, PhD (Louisiana State University) and Charles Hoover, PhD (UCSF, Stomatology and Microbiology), supplied cultures of *P. gingivalis*. Results previously reported in abstract [47].

REFERENCES

1. Neill ME, Melloni JT. Clinical efficacy of the Nd:YAG Laser for combination periodontitis therapy. *Pract Periodontics Aesthet Dent* 1997;9(6 Suppl):1–5.
2. Greenwell H, Harris DM, Pickman K, Burkart J, Parkins F, Myers T. Clinical evaluation of Nd:YAG laser curettage on periodontitis and periodontal pathogens. *J Dent Res* 1999;78:138.
3. Harris DM, Gregg RH, McCarthy DK, Colby LE, Tilt LV. Sulcular debridement with pulsed Nd:YAG. *SPIE Proc* 2002;4610:49–58.
4. Gregg RH, McCarthy DK. Laser ENAP for periodontal bone regeneration. *Dent Today* 1998a;17(5):88–91.
5. Gregg RH, McCarthy DK. Laser ENAP for periodontal ligament (PDL) regeneration. *Dent Today* 1998b;17(11):86–89.
6. Gold SI, Vilardi MA. Pulsed laser beam effects on gingiva. *J Clin Periodontol* 1994;21:391–396.
7. Crespi R, Covani U, Margarone JE, Andreana S. Periodontal tissue regeneration in beagle dogs after laser therapy. *Lasers Surg Med* 1997;21(4):395–402.
8. Yukna RA, Evans GH, Vastardis S, Carr RF. Laser-assisted periodontal regeneration in Humans. *IADR* 2003; 1735 (Abstract).
9. Ben Hatit Y, Blum R, Severin C, Maquin M, Jabro MH. The effects of a pulsed Nd:YAG laser on subgingival bacterial flora and on cementum: An in vivo study. *J Clin Laser Med Surg* 1996;14(3):37–143.
10. Chan Y, Chien R. Bactericidal action of Nd:YAG laser radiation in periodontal pockets. *Proceedings 4th Int'l Congress on Lasers in Dentistry, Singapore*: 1994;185–190.
11. Cobb CM, McCawley TK, Killoy WJ. A preliminary study on the effects of the Nd:YAG laser on root surfaces and microflora in vivo. *J Periodontol* 1992;63:701–707.
12. Gutknecht N, Fischer J, Conrads G, Lampert F. Bactericidal effects of the Nd:YAG lasers in laser supported curettage. *SPIE Proc* 1997;2973:221–226.
13. Hardee MW, Miserendino LJ, Kos W, Walia H. Evaluation of the antibacterial effects of intracanal Nd:YAG laser irradiation. *J Endodont* 1994;20(8):377–380.
14. Klinke T, Klimm W, Gutknecht N. Antibacterial effects of Nd:YAG laser irradiation within root canal dentin. *J Clin Laser Med Surg* 1997;15(1):29–31.
15. Moritz A, Gutknecht N, Doertbudak O, Goharkhay K, Schoop U, Schauer P, Sperr W. Bacterial reduction in periodontal pockets through irradiation with a diode laser: A pilot study. *J Clin Laser Med Surg* 1997;15(11):33–37.
16. Moritz A, Jakolitsch S, Goharkhay K, Schoop U, Kluger W, Malinger R, Sperr W, Georgopoulos A. Morphologic changes correlating to different sensitivities of *Escherichia coli* and *Enterococcus faecalis* to Nd:YAG laser irradiation through dentin. *Lasers Surg Med* 2000;26:250–261.
17. Moritz A, Schoop U, Goharkhay K, Schauer P, Doertbudak O, Wernisch J, Sperr W. Treatment of periodontal pockets with a diode laser. *Lasers Surg Med* 1998;22:302–311.
18. Ramskold LO, Fong CD, Stromberg T. Thermal effects and antibacterial properties of energy levels required to sterilize stained root canals with an Nd:YAG laser. *J Endodont* 1997;23(2):96–100.
19. Rooney J, Midda M, Leeming J. A laboratory investigation of the bactericidal effect of a Nd:YAG laser. *B Dent J* 1994;176:61–64.
20. Tseng P, Liew V, Palmer J. The bactericidal effect of Nd:YAG laser: Preliminary in vitro studies. *Periodontology* 1992;13(1):20–25.
21. White JM, Goodis HE, Cohen JM. Bacterial reduction of contaminated dentin by Nd:YAG laser. *J Dent Res* 1991;70: 412.
22. Whittiers CJ, MacFarlane TW, Mackenzie D, Moseley H, Strang R. The bactericidal activity of pulsed Nd:YAG laser radiation in vitro. *Lasers Med Sci* 1994;9:297–303.
23. Schultz RJ, Harvey GP, Fernandez-Beros ME, Krishnamurthy S, Rodriguez JE, Cabello F. Bactericidal effects of the Nd:YAG laser: In vitro study. *Laser Surg Med* 1986;6:445–448.
24. Tseng P, Gilkeson CF, Palmer J, Liew V. The bactericidal effect of a Nd:YAG laser in vitro. *J Dent Res* 1991;70(4):1991.
25. Walsh JT, Deutsch TF. Er:YAG laser ablation of tissue: Measurement of ablation rates. *Lasers Surg Med* 1989;9:327–337.
26. Wan S, Anderson RR, Parrish JA. Analytical modeling for the optical properties of the skin with in vitro and in vivo applications. *Photochem Photobiol* 1981;34(4):493–499.
27. Sliney DH, Wolbarsht ML. Safety with lasers and other optical sources. New York: Plenum Press; 1980.
28. Kadowaki T, Nakayama K, Okamoto K, Abe N, Baba A, Shi Y, Ratnayake DB, Yamamoto K. *Porphyromonas gingivalis* proteinases as virulence determinants in progression of periodontal diseases. *J Biochem (Tokyo)* 2000;128(2):153–159.
29. Caroline AG, Odusanya BM, Potempa J, Mikolajczyk-Pawlinska J, Travis J. A peptide domain on gingipain R which confers immunity against *Porphyromonas gingivalis* infection in mice. *Infect Immunol* 1998;66(9):4108–4114.
30. Daly CG, Seymour GJ, Kieser JB, Corbet EF. Histological assessment of periodontally involved cementum. *J Clin Periodontol* 1982;9(3):266–274.
31. Celesk RA, McCabe RM, London J. Colonization of the cementum surface of teeth by oral Gram-negative bacteria. *Infect Immunol* 1979;26(1):15–18.
32. Lamont RJ, Jenkinson HF. Life below the gum line: Pathogenic mechanisms of *Porphyromonas gingivalis*. *Microbiol Mol Biol Rev* 1998;62(4):1244–1263.
33. Feuille F, Ebersole JL, Kesavalu L, Stepfen MJ, Holt SC. Mixed infection with *Porphyromonas gingivalis* and *Fusobacterium nucleatum* in a murine lesion model: Potential synergistic effects on virulence. *Infect Immunol* 1996;64(6):2094–2100.
34. Grenier D. Nutritional interactions between two suspected periodontopathogens, *Treponema denticola* and *Porphyromonas gingivalis*. *Infect Immun* 1992;60(12):5298–5301.
35. Lamont RJ, Oda D, Persson RE, Persson GR. Interaction of *Porphyromonas gingivalis* with gingival epithelial cells maintained in culture. *Oral Microbiol Immunol* 1992;7(6):364–367.
36. Deshpande RG, Khan M, Genco CA. Invasion strategies of the oral pathogen *Porphyromonas gingivalis*: Implications for cardiovascular disease. *Invasion Metastasis* 1999;18(2):57–69.
37. Duncan MJ, Nakao S, Skobe Z, Xie H. Interactions of *Porphyromonas gingivalis* with epithelial cells. *Infect Immun* 1993;61(5):2260–2265.
38. Scragg MA, Kelly MJ, Williams DM. *Porphyromonas gingivalis* induces ultrastructural and cytoskeletal changes in adherent human polymorphonuclear leucocytes. *J Submicrosc Cytol Pathol* 2000;32(2):221–228.
39. Leknes KN. The influence of anatomic and iatrogenic root surface characteristics on bacterial colonization and periodontal destruction: A review. *J Periodontol* 1997;68(6):507–516.
40. Adriaens PA, De Boever JA, Loesche WJ. Bacterial invasion in root cementum and radicular dentin of periodontally

- diseased teeth in humans. A reservoir of periodontopathic bacteria. *J Periodontol* 1988b;59(4):222–230.
41. Adriaens PA, Edwards CA, De Boever JA, Loesche WJ. Ultrastructural observations on bacterial invasion in cementum and radicular dentin of periodontally diseased human teeth. *J Periodontol* 1988a;59(8):493–503.
42. Socransky SS, Haffajee AD. Microbial mechanisms in the pathogenesis of destructive periodontal diseases: A critical assessment. *J Periodont Res* 1991;26:195–212.
43. Nalbandian J. The microscopic pattern of tetracycline fluorescence in the cementum of human teeth. *J Biol Buccale* 1978;6(1):27–41.
44. Vahdaty A, Pitt Ford TR, Wilson RF. Efficacy of chlorhexidine in disinfecting dentinal tubules in vitro. *Endod Dent Traumatol* 1993;9(6):243–248.
45. Berutti E, Marini R, Angeretti A. Penetration ability of different irrigants into dentinal tubules. *J Endodont* 1997;23(12):725–727.
46. Lewis K. Minireview: Riddle of biofilm resistance. *Antimicrob Agents Chemother* 2001;45:999–1007.
47. Harris DM, Loomer PM. Ablation of *Porphyromonas gingivalis* in vitro with dental lasers. IADR, San Antonio, March 2003; 855 (Poster).

